Raman spectroscopy and electrical properties of polypyrrole doped dodecylbenzene sulfonic acid/Y_2O_3 composites

M. Irfan[a,*], A. Mustafa[b], A. Shakoor[a], A. N. Niaz[a], N. Anwar[a], M. Imran[c] and A. Majid[d]

[a]*Institute of Physics, Bahauddin Zakariya University, Multan, 60800 Pakistan.*
[*]*e-mail: mirfanphysics@gmail.com*
[b]*Nishtar Medical College University of Health Sciences Lahore Punjab Pakistan.*
[c]*Department of Physics, Govt College University (GCU) of Lahore 54000 Pakistan.*
[d]*Department of Physics, University of Gujrat, Punjab.*

Received 21 April 2023; accepted 18 August 2023

The doped dodecylbenzene sulfonic acid (DBSA) with polypyrrole (PPy) and also incorporated an increasing concentration of Y_2O_3 to obtain the composites of PPy-DBSA-Y_2O_3 via chemical polymerization technique. The PPy-DBSA-Y_2O_3 composites formation were confirmed by interaction between PPy-DBSA and Y_2O_3-particles utilizing Raman spectroscopy. The SEM micrographs show that the composites are in the form of lengthened chains; increase in the particles size as equated with pristine PPy and Y_2O_3 was also studied. Thermal stability of PPy-DBSA- Y_2O_3 composites was improved as enhanced the load of Y_2O_3-particles. The increase in DC conductivity by mixing Y_2O_3 into PPy-DBSA at all temperatures showed the three-dimensional Mott's variable range hopping model. Density of localized states, hopping dimension as well as activation energy are computed and found to be affected due to the presence of Y_2O_3 in DBSA-PPy. The ESR of Y_2O_3 ($\sim$12 Ω), PPy ($\sim$11.80 Ω), PPy-DBSA ($\sim$11.30 Ω) and PPy-DBSA-8%Y_2O_3 composite ($\sim$9.50 Ω). EIS results confirm that the PPy-DBSA-8% Y_2O_3 composite with a low value of impedance gives a maximum value of electrical conductivity.

Keywords: Raman analysis; EIS; PPy-DBSA; Y_2O_3; DC Conductivity.

DOI: https://doi.org/10.31349/RevMexFis.70.010502

1. Introduction

Conjugated polymers have been a significant research area in pure and applied fields since the last two years [1-4]. The conjugated polymer, for example polypyrrole, polyaniline, etc., are polymers with electronically conjugated backbones that, when doped, conduct electricity.

These materials have recently fascinated attention due to their possible use in numerous technological applications that could benefit from their exceptional polymeric and electronic properties [5]. The possible applications of conjugated polymers are the fabrication of solid-state devices, for instance, schottky diodes, microelectronics as well as solar cells. Numerous conjugated polymers possess poor environmental stability and low mechanical properties, owing to which they were not valuable for the fabrication of devices. To minimize these difficulties, many efforts were made to synthesize the conjugated polymer composites to achieve the mechanical properties [6-8]. Some of the variations required to synthesize the hybrid materials provide an organic material through inorganic oxides of various metals, for example, SnO_2 [9], TiO_2 [10], fly ash [11], Fe_3O_4 [12] and ZrO_2 [13] are also mixed conjugated polymers to provides the composites. The study of charge transport mechanism in these composites was a significant part of polymer investigation. Even though a combination of functional dopant like dodecylbenzene sulfonic acid (DBSA) is added into the conjugated polymer, which may distort the polymer chain and produces polarons and bipolarons [14]. Conjugated polymers are very cheap organic semiconductor material having polarons and bipolarons moving charge carriers that are accountable for their electrical conduction and also suitable for the fabrication of electronic devices [15]. The charge transport mechanism taking place in polyacetylene was observed due to the moving solitons [16]. Among various conjugated polymers, the polypyrrole (PPy) is frequently used owing to elevated electrical conductivity and good environmental stability [17]. Among lots of inorganic material, Y_2O_3 has been broadly studied due to its good thermal stability and is mainly used in phosphors host matrices [18] and dielectric insulator of electro-luminescent devices [19-20]. Moreover, Y_2O_3 is a very essential ceramic compound that can be used as a corrosion resistance material, temperature dependent electronic devices fabrication particularly due to high thermal stability. The Y_2O_3 plays very important role in laser host materials to enhance the life span of luminous lamps and their thermal stability [21-22]. Finally, the Y_2O_3 owing to high surface area was utilized as a catalyst carrier [23] in order to increase the conductivity of temperature dependent electronic devices. Until now, a literature review refers to temperature dependent DC conductivity, thermal stability and impedance investigations on PPy-DBSA-Y_2O_3 are unusual. In present work, we report chemical preparation of PPy-DBSA-Y_2O_3 composites, and the prepared material is characterized using Raman spectroscopy, TGA and EIS analysis.

The results cover thermal stability, impedance and temperature dependent DC conductivity; hopping length in addition to activation energy were calculated and discussed the obtained results were valuable for electronic devices fabrication.

2. Experimental details

2.1. Chemicals and material

Pyrrole (Fluka) was refined under reduced pressure and temperature preceding to its usage. Ammonium persulphate, Dodecylbenzene sulfonic acid in addition to Yttrium oxide were purchased (Sigma-Aldrich) utilized as achieved. The whole material was employed as presented without slightly further purification.

2.2. Preparation of PPy and PPy-DBSA-Y_2O_3

The 0.3 mol of Pyrrole was incorporated gradually into the solution which was placed on a magnetic stirrer. While strong stirrers retain the pH value between 0 and 1, 30% HCl was also added into the reaction solution. In this solution, the 0.15 mol of DBSA and Y_2O_3 powder were both dispersed into a reaction mixture under a strong stirrer. In the next hour, the required quantity of ammonium persulphate was dispersed in 100-mL distilled water dropwise under a magnetic stirrer 1/2-hour period. The molar ratio of dopant/ monomer/oxidant was kept 1/4:1:1. At that time, one-liter methanol was mixed into the solution mixture which was kept at 30°C for 48 hours to obtain the entire polymerization. Finally, the solution is cleaned and purified using de-ionized water until the filtrate solution becomes colorless. The greenish-black paste of polypyrrole and PPy-DBSA-Y_2O_3 was achieved by being dehydrated in a vacuum oven at 70°C for 24 hours.

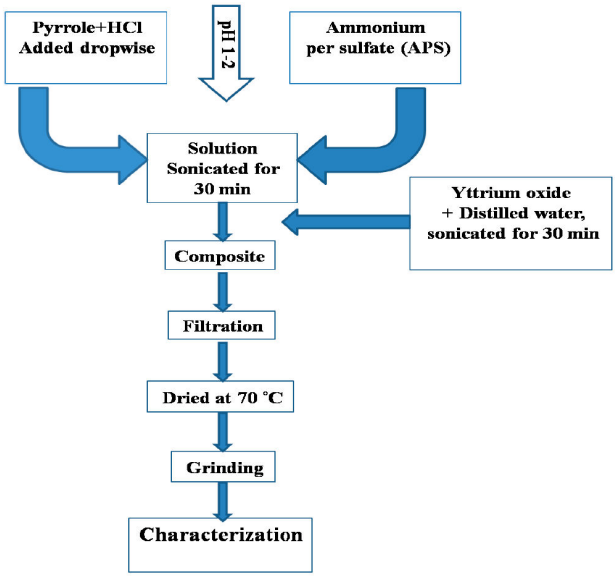

FIGURE 1. Flow chart for the preparation of PPy-DBSA-Y_2O_3 composites by in-situ polymerization process.

3. Measurements

A Renishaw RM 1000 (He-Ne laser) Olympus metallurgical microscope and a CCD detector were utilized for all samples. Scanning electron microscope was carried out on EVO50 ZEISS tool. The thermogravimetric analysis (TGA) was carried out on Mettler thermo balance STAR S.W. 8.10 for all samples. Temperature-dependent DC conductivity for entire samples was executed by Keithley, 2400 electrometers along with the current source electrometer, employing the two-probe method. Electrochemical impedance spectroscopy (EIS) measurements are taken at 0.7 V potential with 0.005 Vrms amplitude in the (10^5 to1) Hz frequency range.

4. Results and discussion

4.1. Raman spectroscopy analysis

Raman spectroscopy was employed to observe structural variations by adding Y_2O_3-particles into DBA-PPy. Figures 2 (a-b) shows the Raman spectra of polypyrrole and DBSA-PPy. The peaks were observed at 1055 cm^{-1} (1060 cm^{-1} for polypyrrole) associated with the polaron quinonoid structure. Moreover, two peaks were observed at 934 cm^{-1} and 1255 cm^{-1} also correlated to bipolaron quinonoid structure that confirmed the doped PPy structure [24]. The peak observed at 1578 cm^1 is a typical quinoid C = C stretched mode of polymer chain. The DBSA-PPy composite with improved bipolarons (1255 cm^{-1}) as equated to polarons in PPy spectra also increased the electrical conductivity [25].

Figures 2 (c-e) shows the Raman spectra of PPy-DBSA-Y_2O_3 by incorporating the various load ratio of Y_2O_3 from 2%, to 8% into PPy-DBSA. The major peaks were observed

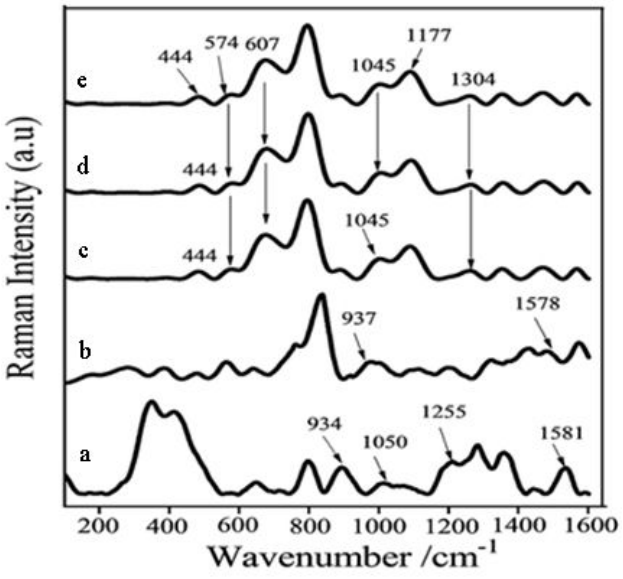

FIGURE 2. Raman spectra of a) pure PPy b) PPy-DBSA c) 2% d) 4% e) 8% load of Y_2O_3 in PPy-DBSA.

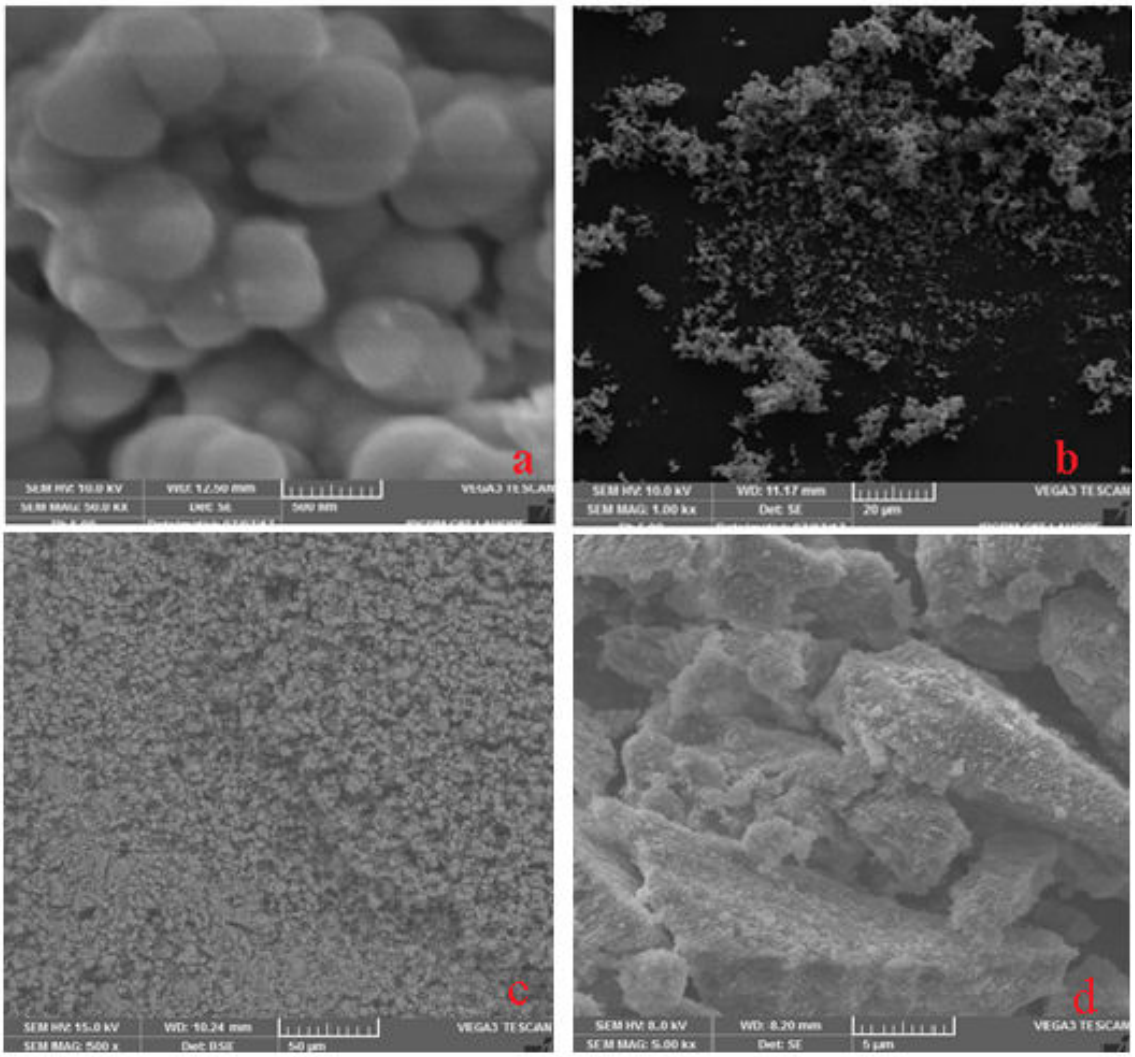

FIGURE 3. Scanning electron micrographs of a) pure PPy b) PPy-DBSA c) PPy-DBSA-8% Y_2O_3 composite d) Y_2O_3.

in PPy-DBSA-Y_2O_3 composites at 1177 cm^{-1} (N-C extending band), 1304 cm^{-1} (C-N extending band), 1045 cm^{-1}(C - H in-plane distortion) as well as pristine Y_2O_3 peak was seen at 444 cm^{-1}. Furthermore, two peaks were also examined at 607 cm^{-1} correlated with distortion in the benzene ring [26] and at 574 cm^{-1} attributed to a cross-link between PPy chains [27]. The peak observed at 607 $cm^{-1}$was identified as distortion of a benzene ring in PPy backbone. Figure 1(e) shows that the intensity of the peak at 607 cm^{-1} increases as compared to the peak observed at 574 cm^{-1} which suggests the confirmation regarding the interactions between the polymer elements. It has been revealed that after mixing the Y_2O_3 presenting the strong interaction between PPy chains was also observed [28]. The comparative intensity of a peak investigated at 607 cm^{-1} shows that PPy-DBSA composite including Y_2O_3-nanoparticles provides a strong interchain interaction. This effect was also observed in the composite that contained 8% load of Y_2O_3. From this investigation, it can be concluded that the induced variations in the observed spectrum of new peaks in all composites confirm the formation of strong interaction between the polymeric chain and Y_2O_3-nanoparticle.

4.2. Scanning electron microscopy (SEM) analysis

Figures 3(a-d) exhibits SEM micrographs of PPy, PPy-DBSA and its PPy-DBSA-Y_2O_3 composite as well as pure Y_2O_3-particles. It was clearly observed from the SEM image of polypyrrole (PPy) that it has bunches of globular shaped particles. The SEM morphology of PPy doped DBSA also shows the cluster of particles which might be due to better inter-chain interaction and consequences to enhance the conductivity [29]. The SEM image is suggestive of the hemispherical nature of polymer as clusters in PPy-DBSA-Y_2O_3 composite and flakier structure of pristine Y_2O_3. The Y_2O_3-particles are encircled into PPy-DBSA chain owing to robust particle-interaction. From this, it may be concluded that PPy-DBSA-Y_2O_3 composite is seeing more progress in particle size and a platelet structure.

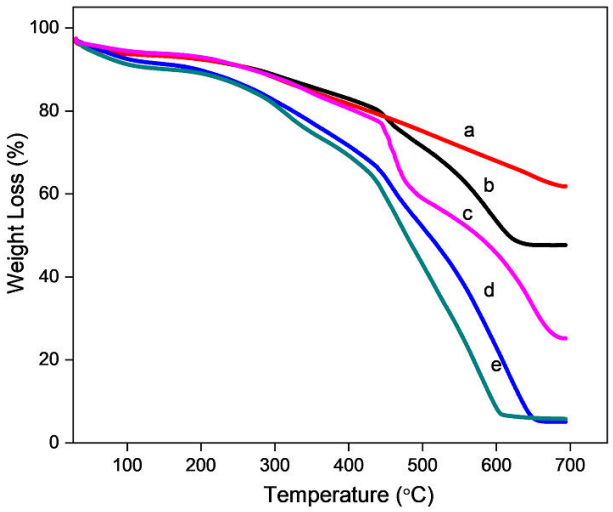

FIGURE 4. TGA of a) PPy b) DBSA-PPy c) 2% d) 4% e) 8% load of Y_2O_3 in PPy-DBSA.

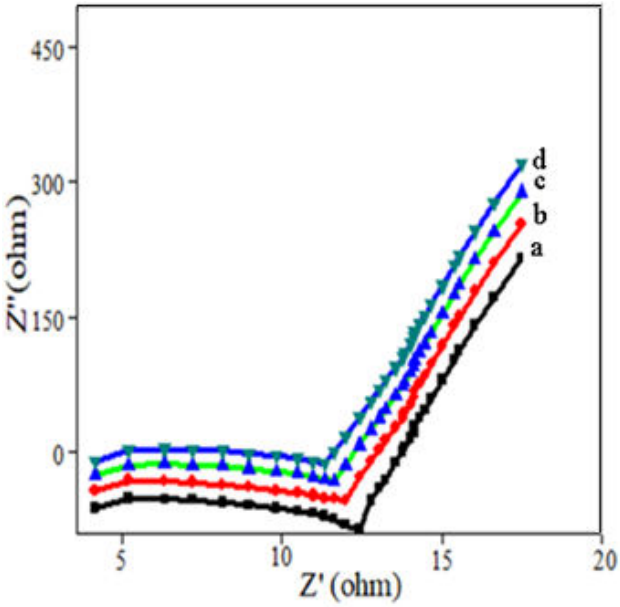

FIGURE 5. Nyquist graphs of a) Y_2O_3 b) PPy c) DBSA-PPy and d) PPy-DBSA-8% Y_2O_3, in 5 mV AC

4.3. Thermogravimetric analysis (TGA)

Figures 4(a-e) shows the typical TGA curves for PPy, DBSA-PPy and their composites with 2% to 8% weight ratio of Y_2O_3 nanoparticles doped in PPy-DBSA. The TGA study shows the two-phase of mass loss: the initial phase ($\sim$100°C) can be permitted humidity desorption from polymer; next phase starts from 230°C to 550°C and it is owing to thermal degradation of the polymer [30]. In comparison to DBSA-PPy, it might be seen that there is no sharp inception of thermal breakdown that occurs at 300°C plotted in the Fig. 4 curve (b). From Fig. 4 curve (e), it can be observed that the mass loss arises in DBSA-PPy-8%Y_2O_3 slowly as compared to pure PPy owing to volatilization of small molecules. Hence, the Y_2O_3 mixed into DBSA-PPy improves thermal stability of all the composites [31].

4.4. Electrochemical impedance analysis

At room temperature, the electrochemical impedance was measured using a 1M-KOH electrolyte and the mass of the sample was chosen (0.01 g). The Nyquist plot of all samples has the vertical line in the high-frequency region, although a semicircle executed in the low-frequency region with a low value of impedance indicates the capacitive nature of all samples [32]. The impedance was measured for all samples with equivalent series resistance (ESR). The ESR of PPy-DBSA-8% Y_2O_3 composite is lower as compared to pure Y_2O_3, PPy, and PPy-DBSA as executed in Figs. 5(a-d). ESR of Y_2O_3 ($\sim$12 Ω), PPy ($\sim$11.80 Ω), PPy-DBSA ($\sim$11.30 Ω) and PPy-DBSA-8% Y_2O_3 composite ($\sim$9.50 Ω).

4.5. Electrical properties

4.5.1. DC conductivity

A series of composites was synthesized to maintain the concentrations of pyrrole-constant but adding an increasing extent of Y_2O_3-nanoparticles into DBSA-PPy. Composites with an increasing quantity of Y_2O_3 produce different conductivity as shown in Fig. 6. The increase in conductivity via the enhancing load of Y_2O_3 can be attributed to decreasing the conductive path because of Y_2O_3 as an insulator nature. The increasing quantity of Y_2O_3 reduces the level of conjugated π-bonds in PPy-DBSA and disorders the polymer chains, which increases the conductivity of composites.

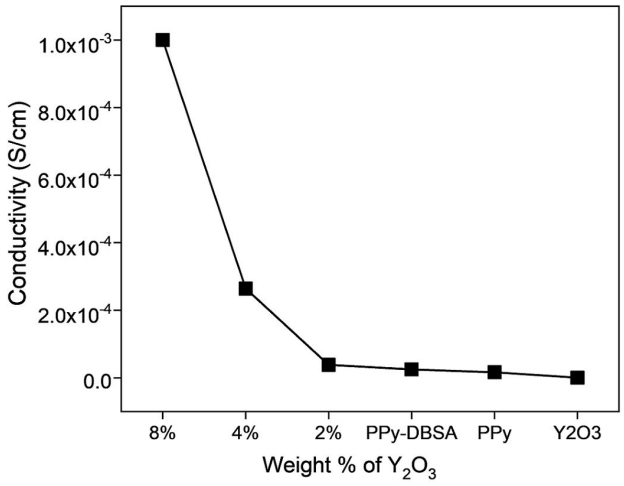

FIGURE 6. Conductivities of PPy-DBSAY_2O_3 composites with different weight % of Y_2O_3.

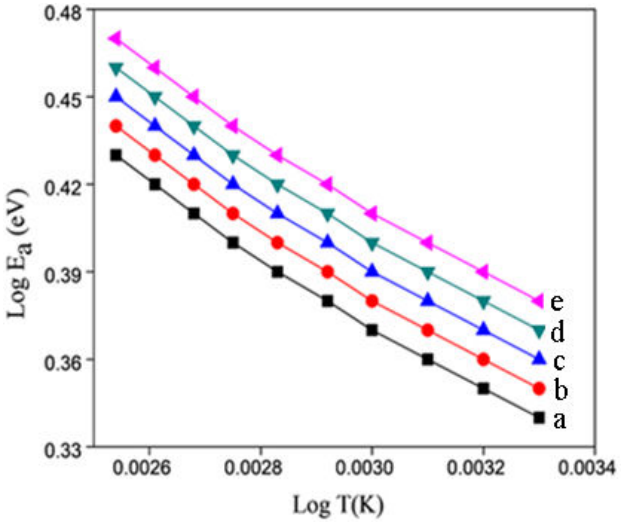

FIGURE 7. Graph of LogE_a against Log$T$ for a) PPy b) PPy-DBSA c) 2% d) 4% e) 8% load of Y_2O_3 in PPy-DBSA composites.

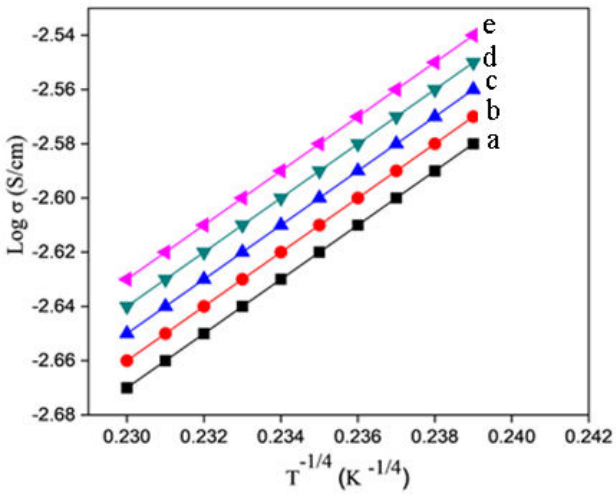

FIGURE 8. Variation in DC conductivity with Temperature for a) PPy b) PPy-DBSA c) 2% d) 4% e) 8% load of Y_2O_3 in PPy-DBSA.

Consequently, Y_2O_3-particles perform an important role in the conductivity of composites.

4.5.2. *Temperature dependant DC conductivity*

The correlation between DC conductivity and temperature for polymer samples may offer significant information about the charge transport mechanism through the polymer scheme. Mott's variable range hopping model adopts the following equations [33-35].

$$\sigma = \sigma_0 \exp\left(T_o/T\right)^{\frac{1}{1+n}} (Scm^{-1}), \tag{1}$$

where n the above expression, $\sigma_0(S.cm^{-1})$ pre-exponential factor is the conductivity of material at the specified temperature T(K), despite T_o(K) Mott's characteristic temperature. The value of σ could be attained from intercepts in addition to slope of Log(σ) plot against $T^{-1/4}$. The following equations can be adopted to calculate the average hopping length [R, cm], density of states [N(E_F), $cm^{-3}eV^{-1}$] as well as hooping activation energy [W, eV] as:

$$\sigma_0 = e^2 R^2 \nu_{ph}\, N \qquad (E_F), \tag{2}$$

$$T_o = \frac{\lambda\alpha^3}{kN(E_F)} \qquad (k), \tag{3}$$

$$R = \left[\frac{9}{8\pi\alpha kTN\left(E_F\right)}\right]^{\frac{1}{4}} \qquad (cm), \tag{4}$$

$$W = \frac{3}{4\pi R^3 N\left(E_F\right)} \qquad (eV). \tag{5}$$

The charge transport mechanism is determined by employing the data in terms of Mott's variable range hopping model. From Eq. (1) exponent n is a dimensionality system, its value $n = 1$, 2 or 3 showing 1, 2 or 3-dimensional variable range hopping charge transport mechanism.

The activation energy Ea is given by Eq. (6):

$$E_a = d(\text{Log}\sigma)/d(1/KT). \tag{6}$$

Therefore, activation energy is calculated from the slope of Log(σ) vs. 1/T and distorted in finding the hopping charge transport mechanism. By using Eqs. (1) and (6), we get the following Eq. (7):

$$E_a = \gamma K T_0 \left(\frac{T_0}{T}\right)^{\gamma - 1} \tag{7}$$

where $\gamma = 1/(1+n)$.

By plotting LogEa vs $\log T$ (Fig. 7) slope of a straight line $-(\gamma - 1)$ equal to 3/4 is attained as the hopping exponent may be $\gamma \sim 1/4$ in addition to $n \sim 3$. This confirmed that the 3-dimensional variable range hopping charge transport mechanism dominates in PPy-DBSA-Y_2O_3 composites, similar to the 3-dimensional variable range hopping charge transport model to pretend in the case of pure PPy. Hence, Log(σ) has a direct relationship with $T - 1/4$ as shown in Fig. 8. The density of localized states decreases whereas hopping length, activation energy as well as σ_{dc} were observed to be increased by the raised load ratio of Y_2O_3. The effective dimensionality n depends upon the interchain coupling of the charge transport mechanism. It can be observed that the charge transport mechanism in conjugated polymers rises via a 3-dimensional variable range hopping model network. The conjugated polymers with various morphology at different temperatures show conductivity data with exponent n either equal to 1/4 [36-38] or 1/2 [39–41] strongly depending on the temperature. The value of the exponent n for temperature dependent DC conductivity is 1/4 and effective dimensionality $n = 3$ [$\gamma = 1/(1+n)$]. Consequently, conductivity data leads to a 3-dimensional variable range hopping model for strong interchain coupling. The value of the exponent n is 1/2 ($n = 1$) and was described in terms of the

TABLE I. Mott's parameters of PPy, PPy-DBSA and PPy-DBSA-Y_2O_3 composites at 303 K.

Samples	T_0 (K)	$N(E_F)$ ($cm^{-3}eV^{-1}$)	R (cm)	W_{hop} (eV)	σ_{dc} (S/cm)
PPy	2.43×10^{11}	3.20×10^{25}	5.90×10^{-9}	0.458	2.30×10^{-4}
PPy-DBSA	3.26×10^{11}	2.40×10^{25}	6.40×10^{-9}	0.450	2.64×10^{-4}
PPy-DBSA-2% Y_2O_3	5.40×10^{11}	1.50×10^{25}	7.30×10^{-9}	0.416	2.76×10^{-3}
PPy-DBSA-4% Y_2O_3	4.30×10^{11}	1.80×10^{25}	6.90×10^{-9}	0.427	2.83×10^{-3}
PPy-DBSA-8% Y_2O_3	3.60×10^{11}	2.20×10^{25}	6.60×10^{-9}	0.436	3.22×10^{-3}

Efros-Shklovskii [41] model or granular metal model [42] variable range hopping in the case of weak interchain coupling. The best fit conductivity data to our synthesized PPy-DBSA-8%Y_2O_3 sample follows the 3-dimensional variable range hopping model. From these outcomes, we found that robust interchain interaction exists in PPy-DBSA-Y_2O_3 composites. However, the reduction in DC conductivity was investigated owing to the insulator nature of Y_2O_3 into DBSA-PPy.

5. Conclusions

PPy-DBSA and also mixed Y_2O_3 nanoparticles have been successfully prepared PPy-DBSA-Y_2O_3 composites utilizing the chemical polymerization route. The structure of prepared samples was explored with Raman spectroscopy. The SEM also confirms the platelet structure in PPy-DBSA-Y_2O_3 composites. The TGA curves confirmed that the thermal stability is increased in all composites by incorporation of the Y_2O_3-particles rather than the pure polymer. The insulator behaviour of Y_2O_3 disrupts delocalization of charge carriers and shrinks the inter-chain coupling, due to which $\sigma_{dc} = 3.20 \times 10^{-3}$ S/cm at 30°C for PPy-DBSA-8%Y_2O_3 is greater as compared to $\sigma_{dc} = 2.70 \times 10^{-3}$ S/cm at 3030°C for PPy-DBSA. The temperature dependent DC conductivity was investigated and the conduction mechanism in these samples follows 3-dimensional variable range hopping model. The ESR of Y_2O_3 ($\sim$12 Ω), PPy ($\sim$11.80 Ω), PPy-DBSA ($\sim$11.30 Ω) and PPy-DBSA-8% Y_2O_3 composite ($\sim$9.50 Ω). Hence, the calculated values of density of localized states, hopping length as well as activation energy are observed to be varied by mixing Y_2O_3-particles into DBSA-PPy.

1. A. Skotheim, Terje, ed. Handbook of conducting polymers 3rd Edition CRC press, **1** (1997) 1-1680.
2. A. J. Heeger, S. Kivelson, J. R. Schrieffer, and W. P. Su, Solitons in conducting polymers. *Reviews of Modern Physics*, **60** (1988) 781.
3. Y. Cao, P. Smith, and A. J. Heeger, Spectroscopic studies of polyaniline in solution and in spin-cast films. *Synthetic Metals*, **32** (1989) 263-281.
4. S. K. Manohar, A. G. MacDiarmid, and A. J. Epstein, Polyaniline: Pernigranile, an isolable intermediate in teh conventional chemical synthesis of emeraldine. *Synthetic Metals*, **41** (1991) 711-714.
5. C. S. Wu, Preparation and characterization of an aromatic polyester/polyaniline composite and its improved counterpart. *Express Polymer Letters*, **6** (2012).
6. M. A. De Paoli, R. J. Waltman, A. F. Diaz, and J. Bargon, An electrically conductive plastic composite derived from polypyrrole and poly (vinyl chloride). *Journal of Polymer Science: Polymer Chemistry Edition*, **23** (1985)1687-1698.
7. N. C. Billingham, and Calvert, P. D. Electrically conducting polymers-a polymer science viewpoint. In Conducting Polymers/Molecular Recognition. Berlin, Heidelberg: Springer Berlin Heidelberg, **1** (2005) 1-104.
8. E. Moons, Conjugated polymer blends: linking film morphology to performance of light emitting diodes and photodiodes. *Journal of Physics: Condensed Matter*, **14** (2002) 12235.
9. A. Bhattacharya, K. M. Ganguly, A. De, and S. Sarkar, A new conducting nanocomposite- PPy-zirconium (IV) oxide. *Materials Research Bulletin*, **31** (1996) 527-530
10. S. J. Su, and N. Kuramoto, Processable polyaniline–titanium dioxide nanocomposites: effect of titanium dioxide on the conductivity. *Synthetic Metals*, **114** (2000)147-153.
11. S. C. Raghavendra, S. Khasim, M. Revanasiddappa, M. V. N. Ambika Prasad, and A. B. Kulkarni, Synthesis, characterization and low frequency ac conduction of polyaniline/fly ash composites. *Bulletin of Materials Science*, **26** (2003) 733-739.
12. W. Chen, X. Li, G. Xue, Z. Wang, and W. Zou, Magnetic and conducting particles: preparation of polypyrrole layer on Fe3O4 nanospheres. *Applied Surface Science*, **218** (2003) 216-222.
13. A. De, A.Das, and S. Lahiri, Heavy ion irradiation on conducting polypyrrole and ZrO2–polypyrrole nanocomposites. *Synthetic Metals*, **144** (2004) 303-307.
14. J. L. Bredas, J. C. Scott, K. Yakushi, and G. B. Street, Polarons and bipolarons in polypyrrole: Evolution of the band structure and optical spectrum upon doing. *Physical Review B*, **30** (1984) 1023.

15. S. R. Elliott, AC conduction in amorphous chalcogenide and pnictide semiconductors. *Advances in Physics*, **36** (1987) 135-217.

16. A. J. Epstein, H. W. Gibson, P. M. Chaikin, W. G. Clark, and G. Grüner, Frequency and electric field dependence of the conductivity of metallic polyacetylene. *Physical Review Letters*, **45** (1980) 1730.

17. X. B. Chen, J. P., Issi, J. Devaux, and D. Billaud, The stability of polypyrrole and its composites. *Journal of Materials Science*, **32** (1997) 1515-1518.

18. K. G. Cho, D. Kumar, P. H. Holloway, and R. K. Singh, Luminescence behavior of pulsed laser deposited Eu: Y2O3 thin film phosphors on sapphire substrates. *Applied Physics Letters*, **73**((1998) 3058-3060.

19. K. Tanabe, M. Misono, Hattori, H., and Ono, Y. New solid acids and bases: their catalytic properties. *Elsevier*, **1** (1990) 1-365.

20. S. Y. Wang, and Z. H. Lu, Preparation of Y2O3 thin films deposited by pulse ultrasonic spray pyrolysis. *Materials Chemistry and Physics*, **78** (2003) 542-545.

21. N. Dasgupta, Krishnamoorthy, R., and Jacob, K. T. Glycol–nitrate combustion synthesis of fine sinter-active yttria. *International Journal of Inorganic Materials*, **3** (2001)143-149.

22. H. D. Wu, L. Lei, Y. G. Jia, and X. Gui, Study on Pyrolysis Behavior of Yttrium Oxalate and Kinetic of Yttria Grain Grown. In Advanced Materials Research,**1**(236) (2011) 1679-1686.

23. S. Roy, W. Sigmund, and F. Aldinger, Grain modification in Y2O3 powders-coarse to nanoporous. Journal of materials science letters, **16** (1997) 1148-1150.

24. S. Demoustier-Champagne, and P. Y. Stavaux, Effect of electrolyte concentration and nature on the morphology and the electrical properties of electropolymerized polypyrrole nanotubules. Chemistry of Materials, **11** (1999) 829-834.

25. S. Gupta, Hydrogen bubble-assisted syntheses of polypyrrole micro/nanostructures using electrochemistry: structural and physical property characterization. Journal of Raman Spectroscopy: An International Journal for Original Work in all Aspects of Raman Spectroscopy, Including Higher Order Processes, and also Brillouin and Rayleigh Scattering, **39** (2008) 1343-1355.

26. Y. Ward, and Y. Mi, The study of miscibility and phase behaviour of phenoxy blends using Raman spectroscopy. Polymer, 40 (1999) 2465-2468.

27. M. Tagowska, B. Palys, and K. Jackowska, Polyaniline nanotubules—anion effect on conformation and oxidation state of polyaniline studied by Raman spectroscopy. Synthetic metals, 142 (2004) 223-229.

28. M. J. L. Santos, A. G. Brolo, and E. M. Girotto, Study of polaron and bipolaron states in polypyrrole by in situ Raman spectroelectrochemistry. Electrochimica acta, **52** (2007) 6141-6145.

29. C. Basavaraja, E. A. Jo,B. S. Kim,D. G. Kim, and D. Huh, S. Electrical conduction mechanism of polypyrrole-alginate polymer films. Macromolecular Research, **18** (2010) 1037-1044.

30. S. Bose, T. Kuila, M. E. Uddin, N. H.Kim, A. K. Lau, and J. H. Lee, In-situ synthesis and characterization of electrically conductive polypyrrole/graphene nanocomposites. Polymer, **51** (2010) 5921-5928.

31. Q. Cheng, V. Pavlinek, C. Li, A. Lengalova, Y. He, and P. Saha, Synthesis and structural properties of polypyrrole/nano-Y2O3 conducting composite. Applied Surface Science, **253** (2006)1736-1740.

32. V. Shaktawat, N. Jain, R. Saxena, N. S. Saxena, and T. P. Sharma, Electrical conductivity and optical band gap studies of polypyrrole doped with different acids. Journal of Optoelectronics and Advanced Materials, **9** (2007) 2130.

33. N. F. Mott, and Davis, E. A. Electronic processes in non-crystalline materials. Oxford university press, **1** (2012) 1-608.

34. A. K. Jonscher, Dielectric relaxation in solids. Journal of Physics D: Applied Physics, **32** (1999) R57.

35. B. Louati, M. Gargouri, K. Guidara, and T. Mhiri, AC electrical properties of the mixed crystal (NH4)3H (SO4)1.42 (SeO4) 0.58. *Journal of Physics and Chemistry of Solids*, **66** (2005) 762-765.

36. R. K. Singh, A. Kumar, and R. Singh, Mechanism of charge transport in poly (2, 5-dimethoxyaniline). *Journal of Applied Physics*, **107** (2010) 113711.

37. A. Elahi, M. Irfan, A. Shakoor, N. A. Niaz, K. Mahmood, and M. Qasim, Effect of loading titanium dioxide on structural, electrical and mechanical properties of polyaniline nanocomposites. *Journal of Alloys and Compounds*, **651** (2015) 328-332.

38. J. Joo,J. K. Lee,J. S. Baeck, K. H. Kim, E. J. Oh, and J. Epstein, Electrical, magnetic, and structural properties of chemically and electrochemically synthesized polypyrroles. *Synthetic metals*, **117** (2001) 45-51.

39. A. Wolter, P. Rannou, J. P. Travers, B. Gilles, and D. Djurado, Model for aging in HCl-protonated polyaniline: structure, conductivity, and composition studies. *Physical review B*, **58** (1998) 7637.

40. Z. H., Wang, E. M., Scherr, A. G. MacDiarmid, and A. Epstein, J. Transport and EPR studies of polyaniline: A quasi-one-dimensional conductor with three-dimensional metallic states. *Physical Review B*, **45** (1992) 4190.

41. T., Hu, and B. I. Shklovskii, Theory of hopping conductivity of a suspension of nanowires in an insulator. *Physical Review B*, **74** (2006) 054205.

42. D. S. Maddison, and T. L. Tansley, Variable range hopping in polypyrrole films of a range of conductivities and preparation methods. *Journal of Applied Physics*, **72** (1992) 4677-4682.